XL CILAMCE
IBERO-LATIN AMERICAN CONGRESS ON COMPUTATIONAL METHODS IN ENGINEERING
NOVEMBER 11-14, 2019
Praiamar Natal Hotel & Convention
Natal, RN-BRAZIL

STUDY OF FLOW AROUND A CIRCULAR CYLINDER - INFLUENCE OF REYNOLDS NUMBER AND TURBULENCE INTENSITY

Leonardo L. V. Rodrigues
leonardo.rodrigues@engenharia.ufjf.br
Graduate Program in Computational Modeling, Federal University of Juiz de Fora
Juiz de Fora, 36036-330, MG, Brazil
Patrícia H. Hallak
patricia.hallak@engenharia.ufjf.br
Department of Applied and Computational Mechanics, Graduate Program in Computational Modeling, Federal University of Juiz de Fora
Juiz de Fora, 36036-330, MG, Brazil

Abstract. Flexible risers, widely used in offshore engineering, are long multilayer tubes designed to carry fluid — such as oil and natural gas — from the seabed to the sea platforms. In this scenario, the risers have to be able to withstand efforts ranging from their weight, water column pressure, to dynamic loads resulting from sea currents. This study aims to evaluate the influence of sea currents on flexible risers. For this interaction, the fluid passage was evaluated in a uniform flow around the cross-section of the tube in a two-dimensional analysis. The seasonality and variation of sea currents over time make it necessary to study different flow regimes. This phenomenon generates pressure variation on the surface structure, causing dynamic efforts that can induce oscillations, increase drag force and cause structural failure if the frequency of vortex shedding approaching one of the natural frequencies in a structure. Therefore, the drag and lift coefficients and Strouhal for Reynolds numbers in the laminar and turbulent regime are so important. They are obtained through modeling using computational fluid dynamics software, ANSYS® Fluent, and then compared with the results of other models in the literature. In the case of the $k - \omega$ SST turbulence model simulations, it is used fixed turbulence intensity values for all Reynolds numbers. This work intends to vary this parameter in order to verify its influence in some aerodynamics coefficients, taking into account the Reynolds number.

Keywords: Vortex shedding, Flexible risers, Computational fluid dynamic, Turbulence intensity, Computational methods.

1 Introduction

Flexible risers, widely used in offshore engineering, are long multilayer tubes designed to carry fluid — such as oil and natural gas — from the seabed to the sea platforms. In this scenario, the risers have to be able to withstand efforts ranging from their weight, water column pressure, to dynamic loads resulting from sea currents.

This study aims to evaluate the influence of sea currents on flexible risers. As for this interaction, the fluid passage was evaluated in an uniform flow around a circular section, miming the cross-section of the tube in a two-dimensional analysis. The motivation for this often comes from the cylindrical geometries used as structures and fluid transport in the offshore industry, like risers that have circular cross-section.

Understanding the flow around a circular cylinder has historically been a fundamental challenge for researchers, largely due to the complexity and transient nature of the wake [1]. That is, The study of a flow around a cylinder has been the object of study for many researchers around the world. One can cite the contribution from Tritton [2] and Dennis and Chang [3] in the middle of the last century. Currently, most of the studies are done using computers, through computational fluid dynamic (CFD) techniques, such as Stringer et al. [1], Abdulaziz [4], Ong et al. [5], Rosetti et al. [6], and many others.

One of the main concern in numerical analysis is to categorize the flow regime, which can range from laminar to turbulent, according with the value of the Reynolds number Re. This important dimensionless quantity express the ratio of inertial forces to viscous forces. In this problem, the boundary layer, free-shear layers, and wake interact and the laminar-turbulent transition and boundary-layer separation move as Reynolds number varies. Also, several instabilities associated with the shear layers play an important role influencing the flow behavior in the different regimes [6].

A notably research from Zdravkovich [7] tried to delimiter the flow regime, according to Reynolds number . A summary of the key stages in flow development is presented in Table 1.

Table 1. Flow regimes around circular cylinder [7]

Re range	Flow regime
$Re < 1$	creeping flow
$3 - 5 < Re < 30 - 40$	Steady separation
$30 - 40 < Re < 150 - 300$	Laminar periodic shedding
$150 - 200 < Re < 1.4 \times 10^5$	Subcritical
$1.4 \times 10^5 < Re < 1 \times 10^6$	Supercritical
$5 \times 10^6 < Re < 8 \times 10^6$	Transcritical
$8\times < Re$	Postcritical

CFD techniques require appropriate modeling of the wide range of turbulence scales since available computer resources are not still able to simulate all of the scales involved in the problem. There are a turbulence modelling strategies [8, 9] and the correct choice among all of them depends on the features of each problem. In this scenario, in line with the objective of this research, the k-ω SST emanates as a prominent model that deserve to be investigated. When setting turbulence parameters it is often necessary to inform the freestream disturbance, which represents the turbulence intensity in the flow.

This use is particularly relevant due to the exploitation of new renewable energies, wind and marine energy technologies, many of which include cylindrical features that need to be assessed for their structural loading caused by vortex shedding.

In following section, the objectives of the research is presented. In Section 3 there is a summary of the continuum mechanics equations. Numerical treatment is detailed in Section 4. Results, discussions

and conclusions are drawn in Section 5 and 6.

2 Objectives

This study aims to use the computational fluid dynamic (CFD) in order to simulate flow around circular cylinder with several Reynolds number, ranging from 10^4, in subcritical regime, to 10^6, in supercritical regime.

The turbulence model was the k-ωSST proposed by Menter [10], Menter et al. [11] implemented in the free version of ANSYS® software [12]. One of the crucial parameters, to set up the simulation, is the specification of transported turbulence quantities quantified by the turbulence intensity [1]. In this situation, the research aims also to evaluate the influence of turbulent intensity variation on control parameters, like drag and lift coefficients and Strouhal number.

We know that low Reynolds number, we have a greater influence of the pressure gradient, and with this study, we want to know which range of Reynolds number has a greater or less influence of turbulence intensity.

3 Theoretical formulation

3.1 Flow model

The flow is predicted by enforcing the conservation of mass and momentum, Eq. 1 and Eq. 2, for viscous and incompressible flow.

- Mass conservation equation

$$\nabla.\vec{v} = 0 \tag{1}$$

- Momentum conservation equation

$$\rho\frac{\partial\vec{v}}{\partial t} + \rho\nabla.\vec{v}\vec{v} = -\nabla.p + \nabla.(\bar{\bar{\tau}}) + \rho\vec{g} + \vec{F} \tag{2}$$

where ρ is the fluid density, p is the static pressure, $\vec{v}$ the velocity field, $\bar{\bar{\tau}} = \mu\left[\left(\nabla\vec{v} + \nabla\vec{v}^T\right)\right]$ is the stress tensor, μ is the viscosity, $\rho\vec{g}$ and $\vec{F}$ are the gravitational body force and external body forces.

3.2 Turbulence modeling

Turbulence is normally present in real flow, and to accurately calculate the turbulent behavior would be very time-consuming and costly, hence turbulence models are often used instead. The most known and popular turbulence models are classified as Reynolds averaged Navier- Stokes (RANS). RANS uses the Reynolds decomposition which says that the variable of interest consists of an average part and a fluctuating part. Thus, the time average of the variable provides the main properties [8].

There are several models within RANS and the most popular family is the two-equation models, namely $k-\varepsilon$ and $k-\omega$ models. In those models, k represents the kinetic energy, ε their dissation and ω the specific rate of dissipation. They all rely on Boussinesq's approximation from 1877 where the stress tensor is modeled in the viscous term of Navier-Stokes Eq. 2. Readers can find in the original references the description of these most popular models [8, 9].

[1] The turbulence intensity relates the root mean square of the turbulent velocity fluctuation and the mean velocity.

In the present work, the original version of k-ωSST turbulence model by Menter [10] is used, where SST stands for shear stress transport. This eddy-viscosity two-equation turbulence model solves one transport equation for the turbulent kinetic energy, k, and one transport equation for the dissipation per unit kinetic energy, ω, also regarded as a turbulent frequency scale [8].

This model is considered to be satisfactory in the treatment of the viscous near-wall region and streamwise pressure gradients, moderate separated flow and the corrections included by Menter [10] resolve some issues of the original model regarding the free-stream flow, blending the best features of the k-ε and the original k-ω.

4 Numerical method

In this section, a detailed account of the setup is given, including boundary, meshing strategy, solver control, and post-processing. We also present some important equations for the withdrawal of data from the simulations.

4.1 Boundary conditions

A sketch up of the computational domain and boundary conditions is presented in Fig. 1.

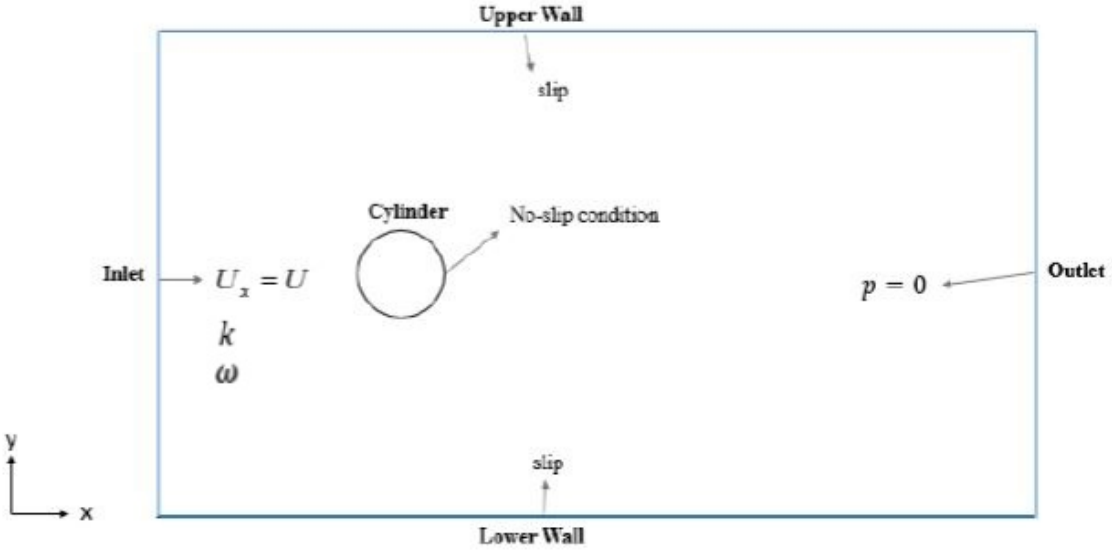

Figure 1. Schematic illustration for boundaries in turbulent flow

The domain width measures 20m and the cylinder is centralized, with a diameter equal to 0.5m. The upstream distance since inlet until the center of cylinder is 8m and from there until the flow output has a distance of 20m.

Also note that the 3rd dimension (z) was set to 1m. In order to ensure a two-dimensional analysis, there is no flow in this direction.

A uniform flow is specified at the inlet, whose Reynolds number is given by Eq. (3), for flow velocity U, where ρ is density of the fluid, D is diameter and μ is dynamic viscosity.

$$Re = \frac{\rho U D}{\mu} \tag{3}$$

This condition, where a fluid is in direct contact with a solid and "sticks" onto the surface, is commonly known as the no-slip condition like Cengel and Cimbala [13]. That is, the cylinder will be set to "no-slip condition", where pressure is set to zero gradient and velocities are set to zero, $U_x = U_y = 0$.

So, the upper and lower wall assigned as "slip" boundaries, shown in Fig. 1, allow the fluid velocity component parallel to the wall to be computed, while velocity normal to the wall is set to zero, $U_y = 0$.

4.2 Turbulence properties

In $k - \omega$ SST model the turbulence variables that need to be specified are turbulence intensity, I, and turbulent viscosity ratio, β. The turbulence intensity I is defined as the ratio of the root-mean-square of the velocity fluctuations, u', to the mean flow velocity, u_{avg}.

$$I = \frac{u'}{u_{\text{avg}}} \tag{4}$$

In CFd is standard practice to select a turbulence intensity from which automatic values are calculated. When setting boundary conditions for a CFD simulation it is often necessary to estimate the turbulence intensity on the inlets. To do this accurately it is good to have some form of measurements or previous experience to base the estimate on. A few examples of common estimations of the incoming turbulence intensity is:[2]

- High-turbulence case: typically the turbulence intensity is between 5% and 20%.
- Medium-turbulence case: flow in not-so-complex devices like large pipes, ventilation flows etc. or low speed flows (low Reynolds number). Typically the turbulence intensity is between 1% and 5%
- Low-turbulence case: flow originating from a fluid that stands still, like external flow across cars, submarines and aircrafts. Very high-quality wind-tunnels can also reach really low turbulence levels. Typically the turbulence intensity is very low, well below 1%.

By setting up the value of I, k and ω parameters are calculated according to the Eq. (5) and Eq. (6).

$$k = \frac{3}{2}(IU)^2 \tag{5}$$

$$\omega = \frac{0.09k}{\beta\nu} \tag{6}$$

Where ν is defined as the ratio between μ and ρ.

4.3 Meshing

The mesh is developed so that the aspect ratio will be higher near the external domain boundaries and smaller near the cylinder. This arrangement is made since the flow is predicted to be a developed flow on that region and is the region with a strong gradient pressure.

The mesh around the cylinder should be finer so that it can generate a more accurate result of simulation.

The model consists of a body fitted hexahedral region surrounding the cylinder with unstructured wedges filling the remaining far field domain.

The mesh/grid near the cylinder is refined by modifying the grading scale and element size in the ANSYS® mesh generator. The mesh can be seen in the Fig. 2. This mesh has 4220 nodes and 6295 elements.

[2] https://www.cfd-online.com/Wiki/Turbulence_intensity

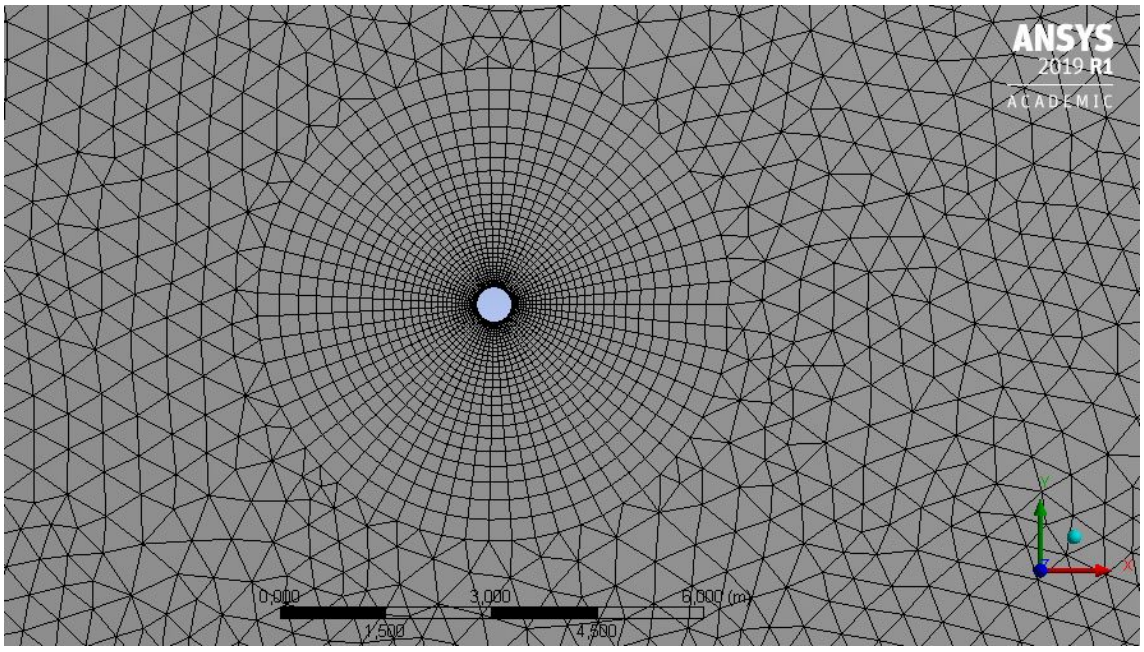

Figure 2. The visualization of the mesh

It is important to note that the lack of any symmetry is theoretically unimportant given sufficient grid resolution, a positive aspect being that it aids the development of vortex shedding for example.

4.4 Solver control

Discretization in finite volume is essential so that all equation terms can be solved. In this work the method of discretization used for gradient was least squares cell based and for the upwind scheme was second order.

The solver that is chosen for turbulent flow simulation in ANSYS® Fluent is explicit formulation.

The result is that a low Courant number is required to maintain numerical stability of which is given in Eq. (7), where Δt is the time step and Δx is the minimum cell width. It was used Courant equal the 0.2 in all cases, since Reynolds number and mesh are same in all cases in this study.

$$Cr = \frac{U\Delta t}{\Delta x} \tag{7}$$

4.5 Post-processing

According to Blazek [14], the force coefficients, such as drag (Cd) and lift (Cl) coefficients on the cylinder, could be extracted from Eq. (8) and Eq. (9), where L is the length of the pipe that the 3rd dimension (z), F_D and F_L are drag and lift force respectively.

$$Cd = \frac{F_D}{0.5\rho LDU^2} \tag{8}$$

$$Cl = \frac{F_L}{0.5\rho LDU^2} \tag{9}$$

The mean drag coefficient, $\overline{C}d$ can be obtained from Eq. (10)

$$\overline{C}d = \frac{\overline{F}_D}{0.5\rho LDU^2} \tag{10}$$

And the lift coefficient amplitude or rms of Cl, $\ddot{C}l$ can be obtained from Eq. (11), where n is the total number of points.

$$\ddot{C}l = \frac{\sqrt{\frac{F_{L_1}^2 + F_{L_2}^2 + ... + F_{L_n}^2}{n}}}{0.5\rho DU^2} \tag{11}$$

The Strouhal number could be extracted from Eq. (12), where f_v is the vortex shedding frequency in Hz.

$$St = \frac{f_v D}{U} \tag{12}$$

The visualization of the simulation results can be seen in the ANSYS® and will be presented at the next session. function

5 Results and discussion

This section presents the results obtained in this study. A comparison with the literature is first performed in order to validate the proposed model. Next, a study of turbulent intensity effects in Strouhal number, drag and lift coefficients for such Reynolds number is presented.

5.1 Validation

To validate the model in ANSYS®, was chosen the case of a turbulent flow on a cylinder for the Reynolds number of 10^4, 10^5 and 10^6. The turbulence parameter was $I = 2.5\%$ and $\beta = 0.075$.

The force coefficients, Cl and Cd as a function of Reynolds number were obtained as result of the simulations.

Figures 3 to Fig. 5 show the average value of the Cd signal, the variation of the rms of Cl signal and the Strouhal number, respectively, with Reynolds number. A comparison with the literature is also provided [1, 7, 15, 16].

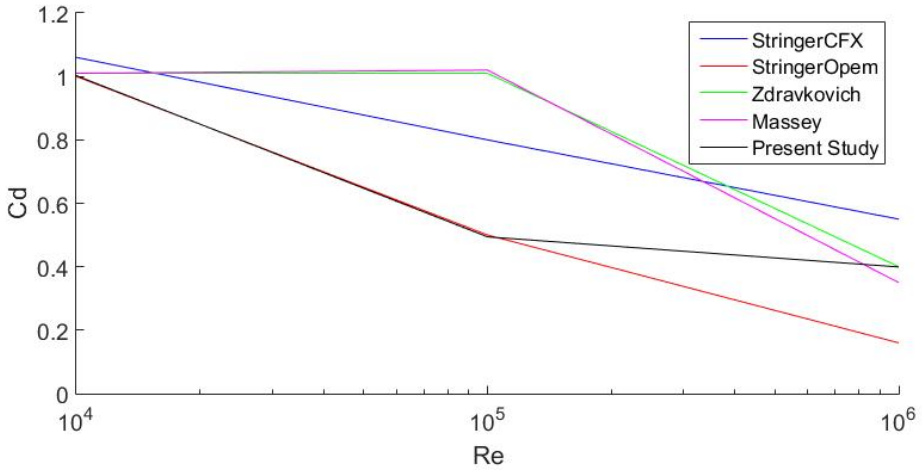

Figure 3. $\overline{C}d$ as function of Re

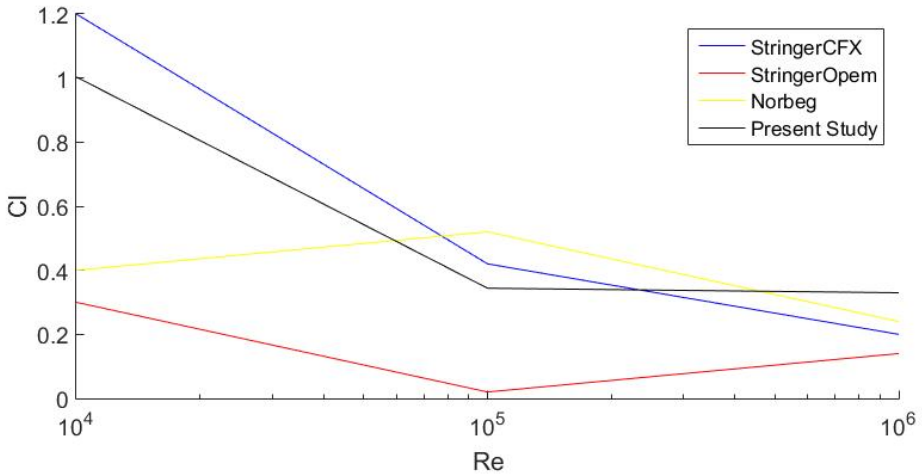

Figure 4. $\ddot{C}l$ as function of Re

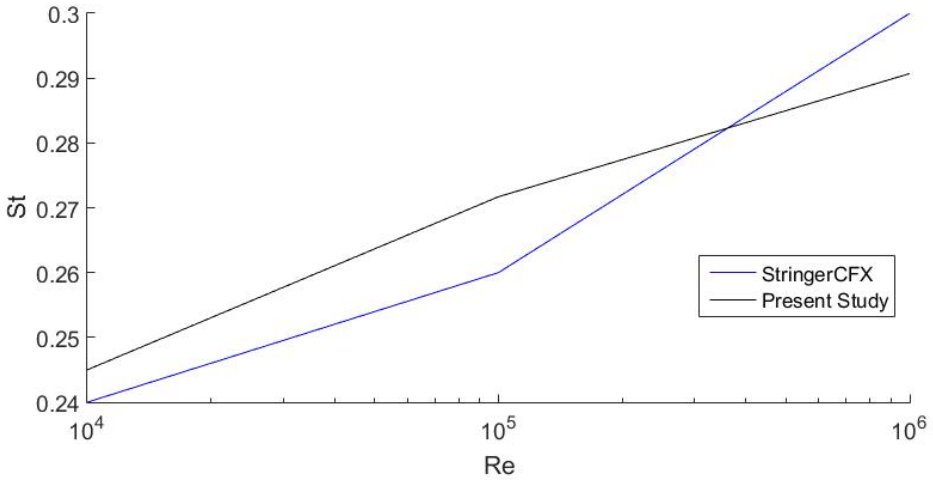

Figure 5. Strouhal number as function of Re

There is a reasonable agreement between the present results with the literature. The behavior of the curves allows some remarks.

- Some authors identified the range $1 \times 10^3 < Re < 2 \times 10^5$ as shear-layer transition regime [6]. In this subcritical regime, the base function increase and the mean recirculation region decreases. These trends are caused by the developing instability of the separating shear layers with an increase in drag, while the point of laminar-turbulent transition in the separating shear layers moves upstream as Re increases [6].
  In the critical transition regime, approximately $2\times10^5 < Re < 5\times10^5$, base function and drag decrease sharply, mainly associated with the separation-reattachment buble, thus making it separate much further downstream and causing a narrower wake than there was so far. This phenomenon is commonly known as drag crisis. At this point, most of the shear layer is turbulent, while the boundary layer is still laminar [6].
  These informations are consistent with present results depicted in Fig. 3 and concise with those presented in Table 1.
- As seem, the rms lift force in Fig. 4 in subcritical regime are widely spread with highly overpredicted values. In the critical region, there is an approach between the results.
  Readers should keep in mind that fluctuating lift is dominated by the actions from the periodic phenomenon called vortex shedding, the principal source of cross-stream flow-induced vibration. However, such modelling needs to take into proper account the supposedly subtle aspects of inherently three-dimensional, transitional and lift-related flow features present in the near-wake [17].

The horizontal velocity profile is presented in Fig. 6 for Re=10^4 and I=2.5%. The velocity profiles will not be presented for all studied cases, since they follow the same trend.

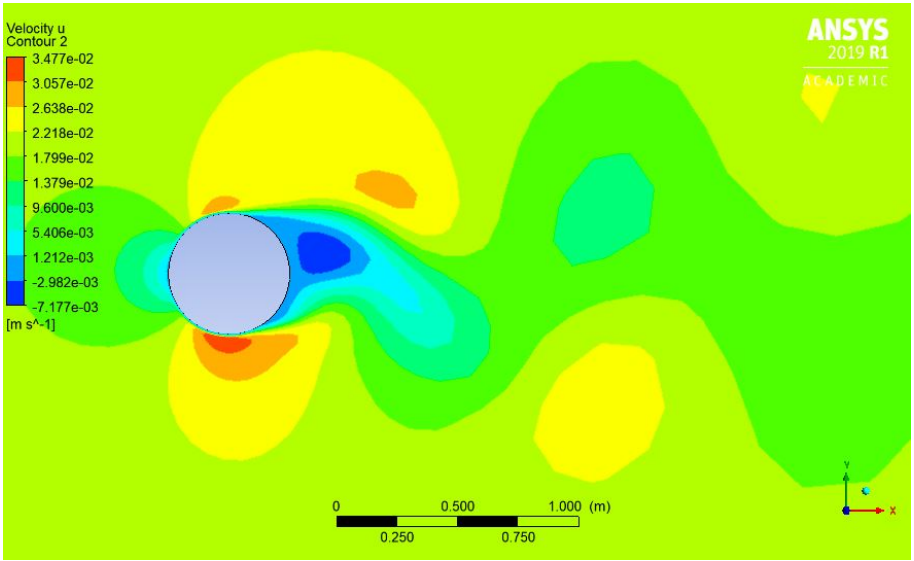

Figure 6. The visualization of horizontal velocity profile for Re=10^4 and I=2.5%

5.2 Turbulence Intensity

This section intends to analyze the influence of turbulence intensity in the aerodynamic parameters. All the features of the simulation were the same from the base case, except the turbulence intensity level. As described in Subsection 4.2, this parameter represents a free stream disturbance in the flow.

Simulations were then performed with Intensity turbulence values of 0.005%, 0.025%, 0.05%, 0.1%, 2.5%, 5% and 10% for each Reynolds numbers of interest, 10^4, 10^5 and 10^6, thus resulting in 21 computer simulations. Simulation results can be seen in Table 2.

Table 2. Simulations result

Re	I(%)	$\overline{C}d$	$\ddot{C}l$	St
10^4	0.005	0.9996	1.0097	0.24
10^4	0.025	0.997	0.9909	0.24
10^4	0.05	1.0002	0.9986	0.245
10^4	0.1	1.005	1.0309	0.245
10^4	2.5	1.0025	1.0035	0.245
10^4	5	0.9976	0.9977	0.24
10^4	10	0.9932	1.0028	0.238
10^5	0.005	0.4899	0.3117	0.272
10^5	0.025	0.49	0.303	0.268
10^5	0.05	0.4917	0.3331	0.269
10^5	0.1	0.4659	0.3527	0.269
10^5	2.5	0.4942	0.3439	0.2717
10^5	5	0.4932	0.3454	0.2717
10^5	10	0.4927	0.3471	0.2717
10^6	0.005	0.3911	0.2676	0.29
10^6	0.025	0.3951	0.2885	0.29
10^6	0.05	0.397	0.2893	0.2907
10^6	0.1	0.3987	0.2988	0.2907
10^6	2.5	0.3993	0.3298	0.2907
10^6	5	0.4019	0.3175	0.2907
10^6	10	0.4009	0.31	0.2907

From the Fig. 7 and Fig. 8 the variation in coefficients caused by the modification of turbulence intensity is not fully evident. However, it is possible to highlight some comments about the results:

- $\overline{C}d$ behavior
  - There is a slight variation of this parameter. Its variation can be quantified by the standard deviation, which was kept in the order of 10^{-3}. This parameter is related with the mean flow and is weakly influenced by freestream disturbance.
  - For $Re = 10^4$ and I 0.1% (midium turbulence level), this parameter reach his maximum. As increasing Re number, the maximum approach the value of maximum I. May be, for low Reynolds of 10^4, flows are more influenced by shear stress layers than by turbulence intensity.
    Norberg [18] also reported the same observation in his text. This author conduct an experimental campaign seeking to evaluate the influence of Reynolds number and turbulence intensity in Strouhal number. According with this authors, " The high sensitivity to freestream disturbances in this range is reflected in the curve for I = 0.1%.".
- $\ddot{C}l$ behavior

  - The most remarkable influence of I was observed in the fluctuation od Cl. The standard deviation increases as Reynolds increases, and was 0.8% , 1.5% and 1.62% for Re 10^4, 10^5 and 10^6, respectively. Ths behavior can be related with the fact that, in general, turbulence models like RANS is worried about modeling the fluctuation of the flow, as a result of Reynolds decomposition.
  - Again, for elevates Re the highest values were observed for high turbulence intensity.
- Strouhal number is associated with the periodicity of Cl signal. Results shown that, for Re 10^4, this value is higher for low I and decreases as I increases. As advancing in Re number, there is a tendency to uniformize this value in a constant value. In others words, for Reynolds number at 10^4 and 10^5 there is a greater variation of Strouhal number when compared to the Reynolds number of 10^6.

  Again, another agreement with Norberg [18] results. Theses researchers reported that in subcritical regime the Strouhal number is dependent on the turbulence intensity.

Data from Table 2 are represented graphically in Fig. 7 to Fig. 15. Variations of the aerodynamic parameters with Reynolds, for all range of I, are shown in Fig. 7 to Fig. 9. Variations of the aerodynamic parameters with I for each Reynolds number are represented in Fig. 10 to Fig. 15.

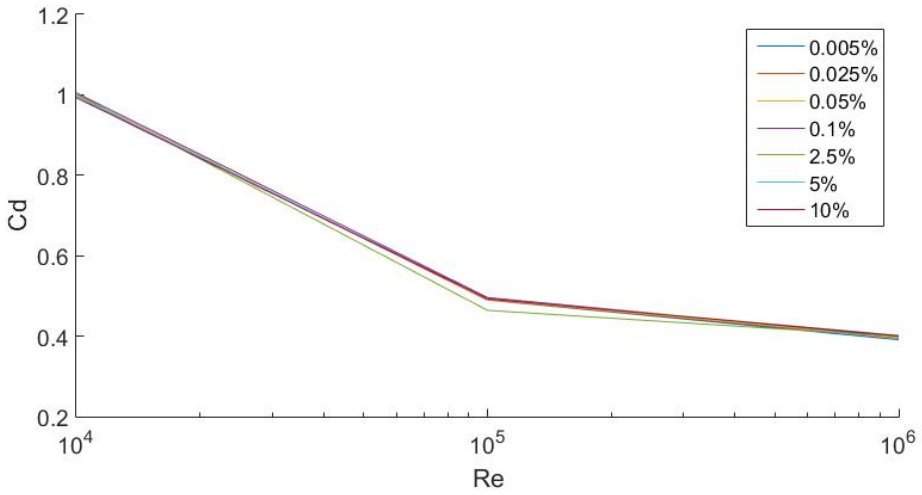

Figure 7. $\overline{C}d$ as function of Re for each turbulence intensity level.

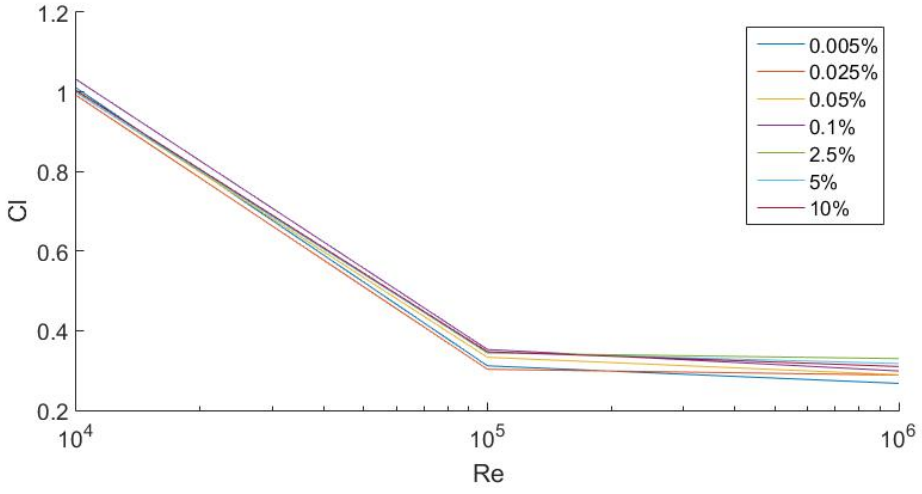

Figure 8. $\ddot{C}l$ as function of Re for each turbulence intensity level.

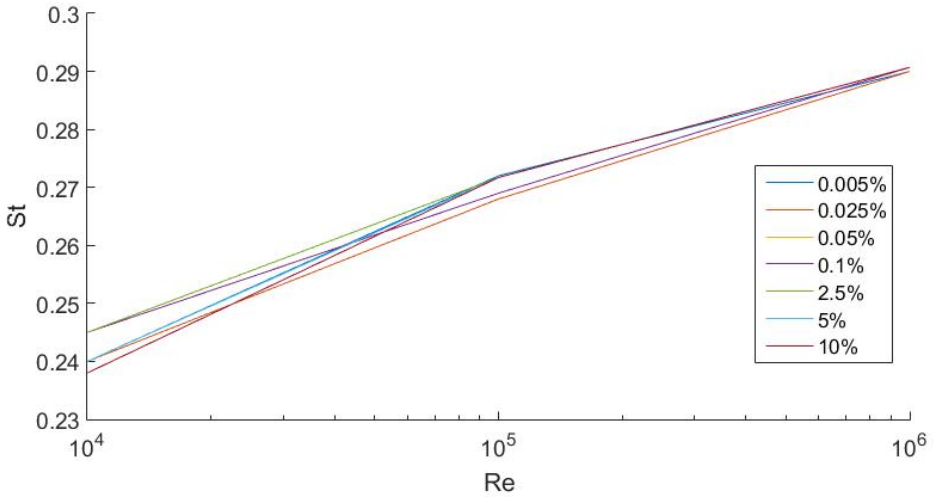

Figure 9. Strouhal number as function of Re for each turbulence intensity level.

In order to better visualize the influence of this parameter on each Reynolds number studied, the following in Fig. 10 to Fig. 12 were generated for Reynolds number of 10^4, 10^5 and 10^6 respectively.

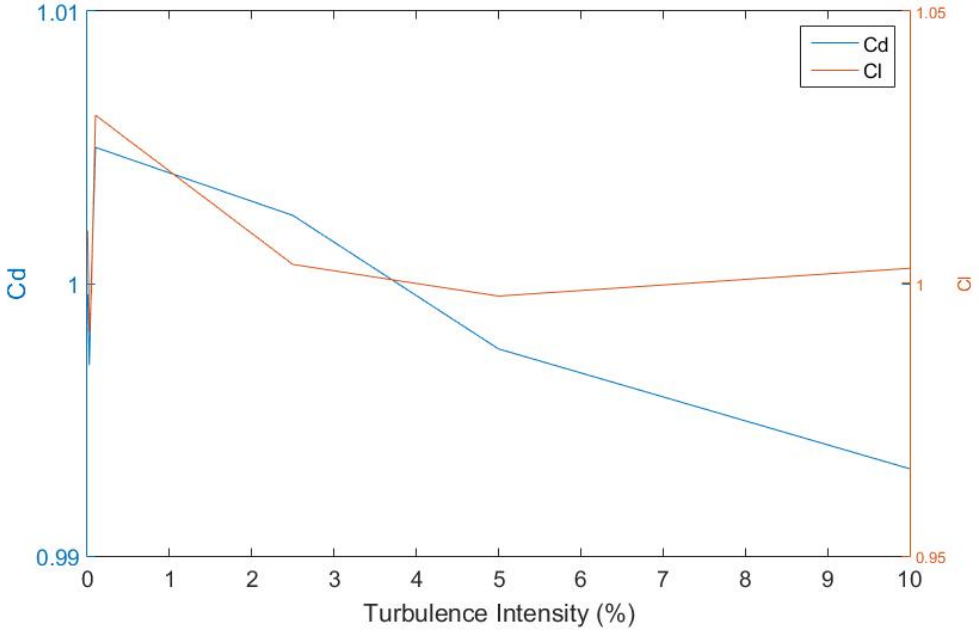

Figure 10. $\overline{C}d$ and $\ddot{C}l$ as function turbulence intensity for Re=10^4

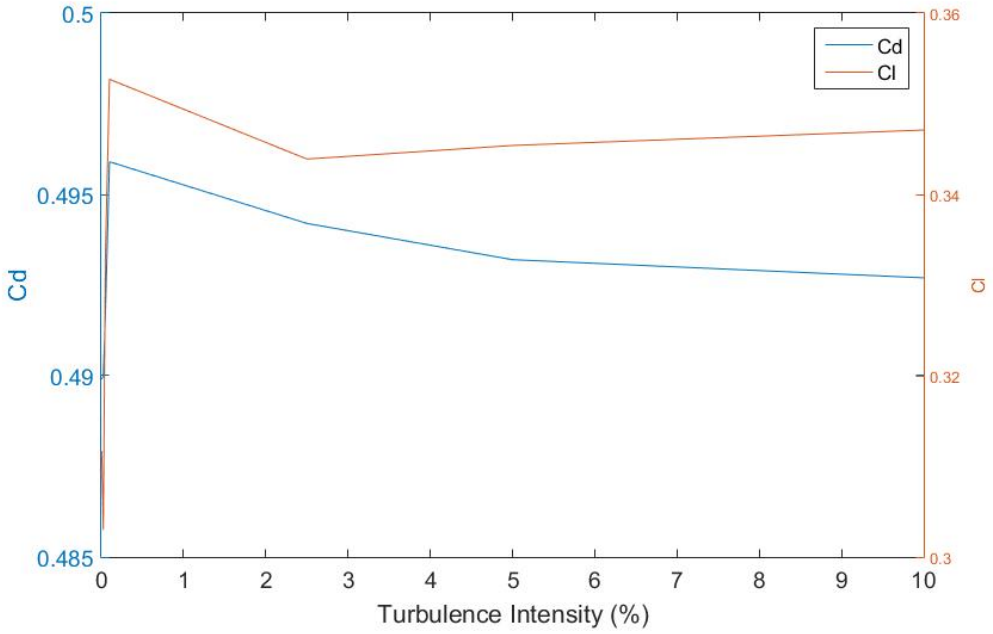

Figure 11. $\overline{C}d$ and $\ddot{C}l$ as function turbulence intensity for Re=10^5

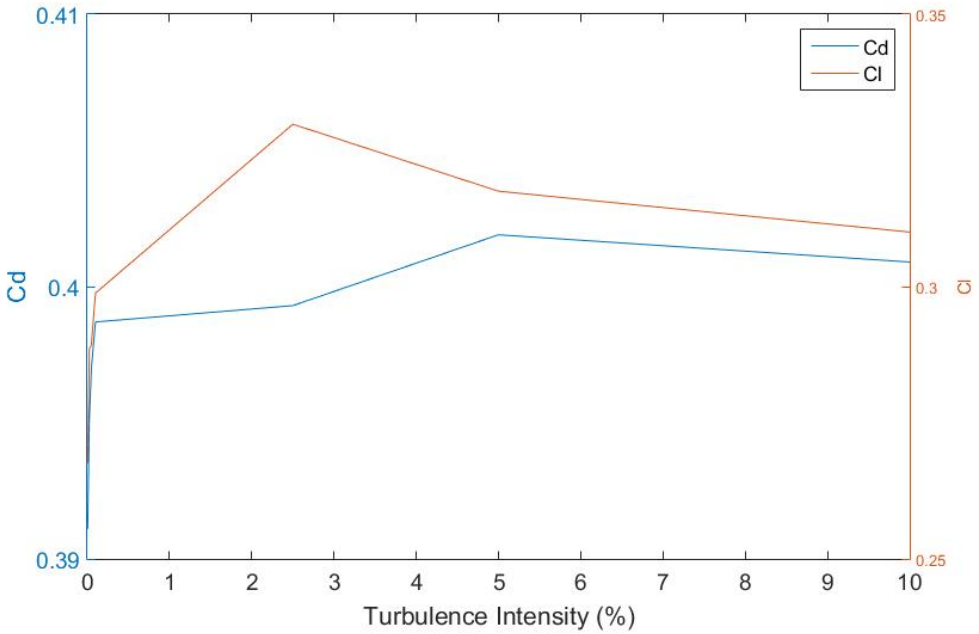

Figure 12. $\overline{C}d$ and $\ddot{C}l$ as function turbulence intensity for Re=10^6

The graphs in relation to the Strouhal as function turbulence intensity are presented in Fig. 13 to Fig. 15 respectively for Reynolds number of 10^4, 10^5 and 10^6, although it was observed low interference of the turbulence intensity for all studied Reynolds numbers.

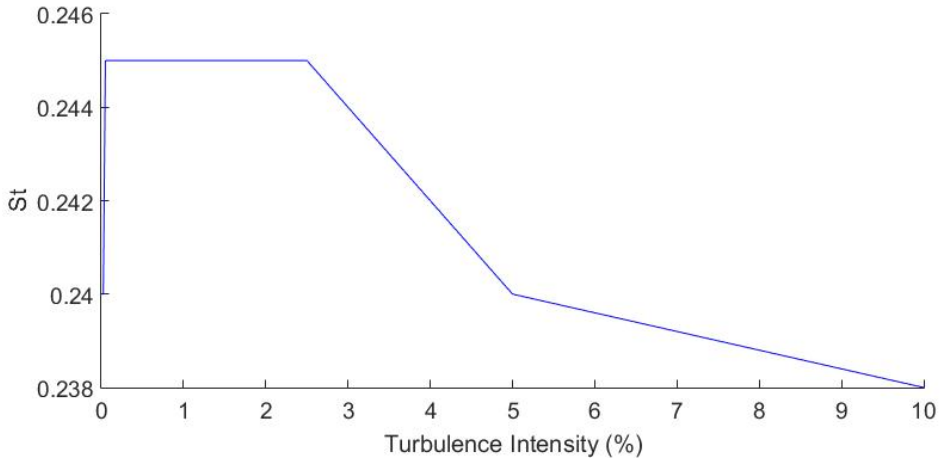

Figure 13. Strouhal number as function turbulence intensity for Re=10^4

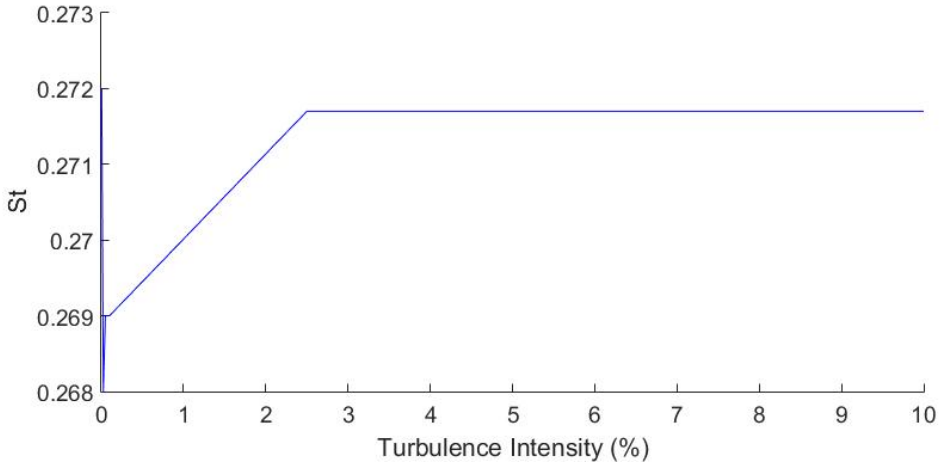

Figure 14. Strouhal number as function turbulence intensity for Re=10^5

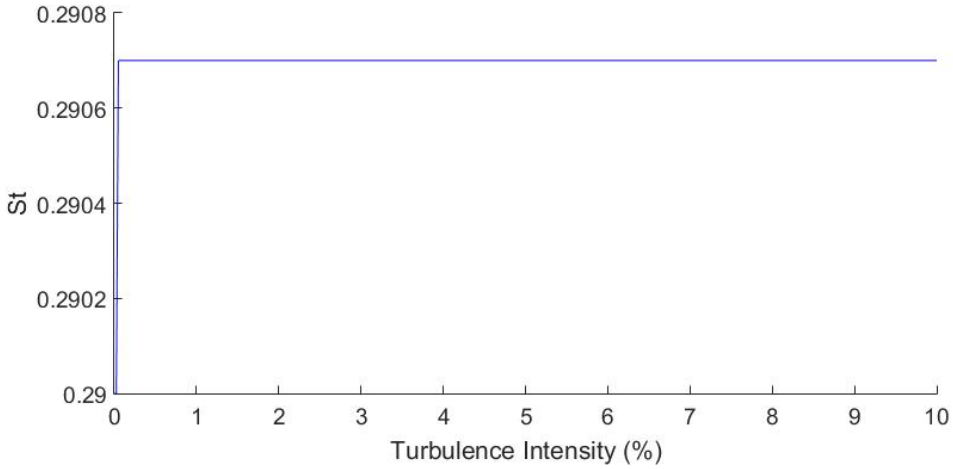

Figure 15. Strouhal number as function turbulence intensity for Re=10^6

6 Conclusions

The objective of this work was satisfactorily achieved. First, the values of $\overline{C}d$, $\ddot{C}l$ and St for the base case converse well with some experimental cases in the literature, as well as with other numerical cases in past studies.

In this way, the modeling done on ANSYS® fluent could be considered as good when compared to other applied numerical methods in previous research and other software.

After that, we conclude that there is an influence of turbulence intensity in the studied parameters, but that influence increases proportionally to the increase in the Reynolds number of the simulation. Like explained in detail in the previous section.

In general, it can be concluded that there is a considerable influence of turbulence intensity in lift coefficient and Strouhal number. For drag coefficient, this influence is very low for every Reynolds number interval studied.

Thus, it is known which coefficients are most influenced by the parameter studied here. And with this, it will be possible to arrive at modeling closer to real cases of the offshore industry, like risers for example. Over the course of the studies, it will become increasingly evident and relevant to analyze the parameters studied here when executing a project involving risers.

This study contributes by identifying which of the studied parameters (Strouhal number, drag and lift coefficient) have a greater or lesser influence on the variation of turbulence intensity.

As future works, and as a way to improve the work in question, we will try to make a comparison of this model with other turbulence models and computational methods or other geometries as an object of study.

Acknowledgements

I thank the postgraduate program in computational modeling at the Federal University of Juiz de Fora and the Coordenação de Aperfeiçoamento de Pessoal de Nível Superior (CAPES) for all the structure and support available.

References

[1] Stringer, R., Zang, J., & Hillis, A., 2014. Unsteady rans computations of flow around a circular cylinder for a wide range of reynolds numbers. *International Journal for Numerical Methods in Engineering*, vol. 87, pp. 1–9.

[2] Tritton, D., 1959. Experiments on the flow past a circular cylinder at low reynolds numbers. *International Journal for Numerical Methods in Engineering*, vol. 6, pp. 547–567.

[3] Dennis, S. & Chang, G., 1970. Numerical solutions for steady flow past a circular cylinder at reynolds numbers up to 100. *International Journal for Numerical Methods in Engineering*, vol. 42, pp. 471–489.

[4] Abdulaziz, M., 2017. *Study of the vortex-induced vibrations in off-shore structures*. PhD thesis, Institute of Ship Technology, Ocean Engineering and Transport Systems (ISMT).

[5] Ong, M. C., Utnes, T., Holmedal, L. E., Myrhaug, D., & Pettersen, B., 2009. Numerical simulation of flow around a smooth circular cylinder at very high reynolds numbers. *Marine Structures*, vol. 22, n. 2, pp. 142–153.

[6] Rosetti, G. F., Vaz, G., & Fujarra, A. L., 2012. Urans calculations for smooth circular cylinder flow in a wide range of reynolds numbers: solution verification and validation. *Journal of Fluids Engineering*, vol. 134, n. 12, pp. 121103.

[7] Zdravkovich, M., 1990. Conceptual overview of laminar and turbulent flows past smooth and rough circular cylinders. *International Journal for Numerical Methods in Engineering*, vol. 33, pp. 53–62.

[8] Wilcox, D. C. et al., 1998. *Turbulence modeling for CFD*, volume 2. DCW industries La Canada, CA.

[9] Pope, S. B., 2001. Turbulent flows.

[10] Menter, F., 1993. Zonal two equation kw turbulence models for aerodynamic flows. In *23rd fluid dynamics, plasmadynamics, and lasers conference*, pp. 2906.

[11] Menter, F. R., Kuntz, M., & Langtry, R., 2003. Ten years of industrial experience with the sst turbulence model. *Turbulence, heat and mass transfer*, vol. 4, n. 1, pp. 625–632.

[12] Fluent, A., 2011. 14.0 user's manual. *ANSYS Inc., Canonsburg, PA*.

[13] Cengel, Y. A. & Cimbala, J. M., 2014. *Fluid mechanics: Fundamentals and applications*, volume III. McGraw Hill.

[14] Blazek, J., 2015. *Computational Fluid Dynamics: Principles and Applications*, volume III. Elsevier.

[15] Massey, B. & Ward-Smith, J., 2006. *Mechanics of fluids*, volume VIII. Elsevier.

[16] Norberg, C., 2003. Fluctuating lift on a circular cylinder: review and new measurements. *International Journal for Numerical Methods in Engineering*, vol. 17, pp. 57–96.

[17] Norberg, C., 2001. Flow around a circular cylinder: aspects of fluctuating lift. *Journal of Fluids and Structures*, vol. 15, n. 3-4, pp. 459–469.

[18] Norberg, C., 1987. Effects of reynolds number and a low-intensity freestream turbulence on the flow around a circular cylinder. *Chalmers University, Goteborg, Sweden, Technological Publications*, vol. 87, n. 2, pp. 1–55.